MUCINOUS CARCINOMA UPREGULATES TARGETS OF SMALL MOLECULE INHIBITORS OF CANCERS: IMPLICATIONS FOR TARGETING ONCOGENIC MUCINS IN THE COLORECTAL CANCER MICROENVIRONMENT

Henry Okuchukwu Ebili[1*], Adesoji Ebenezer Adetona[1], Patrick Akintunde Akintola[1], Uchenna Simon Ezenkwa[2], Adeyinka Kazeem Adegboyejo[3], Ayotunde O. Ale[4], Yusuf Abdullahi[5]

1- Morbid Anatomy and Histopathology Department, Olabisi Onabanjo University, Sagamu Campus, Hospital Road, Sagamu, Ogun State, Nigeria
2- Department of Anatomic Pathology, Federal University of Health Sciences Azare, Bauchi State, Nigeria
3- Department of Medical Microbiology, Faculty of Basic Clinical Sciences, Olabisi Onabanjo University, Sagamu Campus, Hospital Road, Sagamu, Ogun State, Nigeria
4- Department of Medicine, Faculty of Clinical Sciences, Olabisi Onabanjo University, Sagamu Campus, Hospital Road, Sagamu, Ogun State, Nigeria
5- Department of Histopathology, Gombe State University, Tudun Wada, Gombe, Gombe State, Nigeria

Corresponding Author: Henry O. Ebili, Morbid Anatomy and Histopathology Department, Olabisi Onabanjo University, Sagamu Campus, Hospital Road, Sagamu, Ogun State, Nigeria ebili.henry@oouagoiwoye.edu.ng

Citation: Ebili HO, Adetona AE, Akintola PA, Ezenkwa US, Adegboyejo AK, Ale AO, Abdullahi Y. Mucinous carcinoma upregulates targets of small molecule inhibitors of cancers: implications for targeting oncogenic mucins in the colorectal cancer microenvironment. Niger J Oncol 2026;2(2): 219- 241

ABSTRACT

Background: Mucinous colorectal carcinoma (CRC) is a distinct histological subtype characterized by abundant extracellular mucin production and a complex tumour microenvironment (TME). The biological and therapeutic implications of mucin expression in CRC remain incompletely characterized.

Objectives: This study aimed to characterize the transcriptomic landscape, signalling pathway enrichment, and drug-perturbation signatures associated with mucinous CRC, and to investigate whether mucin-associated proteins are functionally integrated into enriched signalling networks.

Methods: Clinicopathological and genomic data from three CRC cohorts (TCGA, Sidra-LUMC, CPTAC2; n=984) were analysed. Mucinous histology was validated using mucin gene-expression signatures. Differential expression, Gene Set Enrichment Analysis (GSEA), Gene Ontology and Pathway Ontology Enrichment Analyses were performed. Protein–protein interaction (PPI) networks were constructed using STRING and analysed in Cytoscape to assess mucin–pathway integration. Drug Ontology Enrichment Analysis (DOEA) was performed using LINCS L1000 Chem

Pert libraries, with preferential enrichment assessed by Differential Ontology Enrichment Frequency (DOEF) and Odds Ratio (DOOR) analyses.

Results: Mucinous carcinomas exhibited significant upregulation of secretory mucin genes (*MUC2, FCGBP, AGR2, AGR3, SPINK4* and *CLCA1*) and enrichment of inflammatory, stromal, hypoxic and angiogenic programmes. PPI analysis demonstrated selective incorporation of mucin-associated proteins into inflammation/chemokine, TLR, T-cell activation and p53 feedback-loop signalling networks, while remaining segregated from integrin and PDGF pathways. DOEA revealed preferential enrichment of calcium channel blocker, mucolytic, N-glycosylation inhibitor and bosutinib transcriptional signatures in mucinous CRC.

Conclusion: Mucinous colorectal carcinoma possesses a distinctive TME characterized by inflammatory, immune and stress-response signalling, with mucin-associated proteins selectively integrated into these networks. The enrichment of anti-mucin drug-perturbation signatures provides a rationale for further experimental investigation of candidate therapeutic strategies targeting mucin production, secretion and glycosylation in this histological subtype.

Keywords: Mucinous Colorectal Carcinoma, Tumour Microenvironment, Mucin, Protein–Protein Interaction, Drug Ontology Enrichment, Small Molecule Inhibitors

INTRODUCTION

Colorectal cancer (CRC) remains a major global health problem, ranking as the third most commonly diagnosed cancer and the second leading cause of cancer-related mortality worldwide.[1-3] Despite substantial advances in diagnosis and treatment, its burden remains high, underscoring the need for a better understanding of CRC biology.[4] In this study, we investigated the tumour microenvironment (TME) of CRC, with particular emphasis on the biological and therapeutic relevance of mucin expression.

Mucinous colorectal carcinoma is a distinct histological subtype characterized by extracellular mucin comprising >50% of the tumour volume.[5] It accounts for 10–25% of CRCs and is commonly associated with right-sided location, younger age, female sex, advanced stage, impaired response to conventional chemotherapy, and poorer prognosis than non-mucinous carcinoma.[5-7] Interest in targeting mucins has increased because the mucin barrier protects tumour cells from therapeutic agents, and disruption of this barrier may improve treatment efficacy.[8-11] Secreted gel-forming mucins undergo extensive glycosylation in the endoplasmic reticulum and Golgi apparatus before secretion,[12-14] while mucin secretion is regulated by sodium-calcium exchanger 2 (NCX2) acting in concert with transient receptor potential melastatin channels TRPM4 and TRPM5.[15,16]

Small-molecule inhibitors (SMIs) comprise diverse compounds (<500 Da) that modulate multiple cancer-related proteins and pathways.[17,18] Their favourable pharmacological properties, including oral bioavailability, tissue penetration, and broad target spectrum, make them attractive therapeutic candidates.[17,18] In the present study, we investigated the transcriptomic and signalling characteristics of mucinous colorectal carcinoma and explored their transcriptional associations with drug-response signatures related to candidate anti-mucin strategies, including calcium channel

blockers (CCBs), mucolytics, N-glycosylation inhibitors (NLGis), and Bosutinib.

The overall aim of this study was to characterize the biological and therapeutic landscape of mucinous colorectal carcinoma using integrated multi-cohort transcriptomic analyses. Specifically, we sought to (i) validate the biological relevance of annotated mucinous histology using mucin gene-expression signatures; (ii) identify differentially expressed genes and signalling pathways associated with mucinous carcinoma; (iii) investigate pathway and drug-perturbation signature correlates of mucinous CRC; and (iv) generate candidate anti-mucin therapeutic hypotheses for future experimental investigation. Given the paucity of comprehensive transcriptomic studies examining the TME and anti-mucin therapeutic signatures in mucinous CRC, this study provides an integrated framework for understanding the biology of this histological subtype.

MATERIALS AND METHODS

Cancer cohorts

This study retrospectively analysed clinicopathological and genomic data (RNA-Seq and copy number segments) from three colorectal cancer (CRC) cohorts: The Cancer Genome Atlas (TCGA),[19] the Sidra-Leiden University Medical Center Atlas and Compass of Immune-Cancer-Microbiome (Sidra-LUMC),[20] and the Clinical Proteomic Tumor Analysis Consortium 2 (CPTAC2),[21] all accessed via the Genome Data Commons and cBioPortal for Cancer Genomics databases.[22,23]

Data retrieval and processing

Clinical, copy number, and gene expression data were retrieved from the three cohorts. Gene expression data were harmonised by gene symbol matching, retaining only genes shared across all cohorts. To minimise cohort-specific technical variation, the combined transcriptomic dataset underwent batch correction using the ComBat empirical Bayes algorithm,[24] with performance assessed by principal component analysis (Supplementary Figure 1). Chromosomal instability indices (Fraction Genome Altered and Aneuploidy scores) were derived from copy number segment files.

Validation of mucinous histology and differential expression analysis

Three single-sample Gene Set Enrichment Analysis (ssGSEA) scores (mucosecretory signature, membrane mucin signature and composite mucin signature) were computed using a curated mucin-associated gene set (*MUC1, MUC2, MUC4, MUC12, MUC13, MUC20, FCGBP, AGR2, AGR3, SPINK4, CLCA1*) selected from published studies of intestinal goblet-cell biology, secreted mucins and mucinous colorectal carcinoma.[25-27] The score was computed to validate the annotated mucinous histology. Differential expression (DE) analysis was performed on the ComBat-corrected dataset using the limma package,[28] with histological classification as the phenotype variable. Differentially expressed genes were defined using FDR-adjusted $P < 0.05$ and absolute $\log_2$ fold-change ≥ 0.1.

Gene set and ontology enrichment analyses

Gene Set Enrichment Analysis (GSEA) was performed using GSEA v4.3.3 with annotated mucinous histology as the phenotype label.

Genes were ranked by the Signal2Noise metric, with 1,000 gene-set permutations. Gene sets with nominal $P < 0.05$ and FDR < 0.25 were considered significantly enriched.[29,30] Gene Ontology Enrichment Analysis (GOEA), Pathway Ontology Enrichment Analysis (POEA) using GO Biological Process 2026 and Panther 2016, and Drug Ontology Enrichment Analysis (DOEA) using LINCS L1000 Chem Pert libraries were performed via Enrichr platform (https://maayanlab.cloud/Enrichr).[31] DOEA focused on transcriptional signatures associated with mucolytics, calcium channel blockers, *N*-glycosylation inhibitors, and bosutinib.

Preferential ontology enrichment analyses

Differential ontology enrichment frequency (DOEF) analysis compared the number of significantly enriched ontology terms between mucinous and non-mucinous colorectal carcinomas within each ontology category. Differential ontology odds ratio (DOOR) analysis compared the enrichment odds ratios of shared ontology terms between the two histological subtypes. Because Enrichr reports enrichment odds ratios based on Fisher's exact test, 2 × 2 contingency tables were reconstructed from the overlapping gene counts (gene fraction numerators), annotated gene-set sizes (gene fraction denominators), the input gene list (1,000 genes per subtype), and the Enrichr background (20,000 genes). For each ontology term, a = overlapping genes; b = annotated gene-set size − a; c = 1,000 − a; and d = 20,000 − annotated gene-set size − 1,000 + a. Enrichment odds ratios were calculated as:

$$OR = (a \times d) / (b \times c)$$

The standard error of the natural logarithm of the odds ratio was calculated as:

$$SE = \sqrt{[(1/a) + (1/b) + (1/c) + (1/d)]}$$

The differential odds ratio z statistic was then calculated as:

$$DOOR\ z\ score = [\ln(ORM) - \ln(ORNM)] / \sqrt{(SEM^2 + SENM^2)}$$

where OR and SE denote the enrichment odds ratios and standard errors for mucinous (M) and non-mucinous (NM) carcinomas, respectively. Positive and negative z scores indicated preferential enrichment in mucinous and non-mucinous carcinomas, respectively. DOEF and DOOR analyses were performed in Microsoft Excel (Microsoft Corporation, Redmond, WA, USA). Two-tailed P values were obtained from the standard normal distribution using the Social Science Statistics online calculators (https://www.socscistatistics.com), with $P < 0.05$ considered statistically significant.

Protein–protein interaction analyses

Protein–protein interaction (PPI) analysis was performed using STRING (minimum interaction score ≥0.400), which evaluates whether the observed network contains more interactions than expected for a random protein set of the same size.[32] To assess whether mucin-associated proteins are incorporated into enriched signalling networks, protein–protein interaction (PPI) analysis was performed using STRING (minimum interaction score ≥ 0.400)[32]. A curated mucin-associated gene set (*MUC2, MUC5AC, MUC6, CLCA1, FCGBP, AGR2, AGR3* and *SPINK4*) was combined with genes from significantly enriched Panther 2016 pathways for the PPI analyses. The STRING network file was imported into Cytoscape, where topology was

evaluated using Network Analyzer (degree and betweenness centrality), and functional modules were identified using MCODECLUSTER.[33]

Statistical analyses and data visualization

Relationships between mucinous histology and clinicopathological/molecular variables were analysed using SPSS v29. Categorical variables were compared using Chi-square or Fisher's exact tests, continuous variables with bivariate correlation or one-way ANOVA. Survival was assessed using Kaplan–Meier and Cox regression. GSEA used 1,000 gene-set permutations with default thresholds (nominal $P < 0.05$, FDR < 0.25). Benjamini–Hochberg correction was applied to all analyses, where applicable, with FDR < 0.05. Figures were generated using SR Plot,[30] SPSS, and STRING.[29]

General study approach

We first validated the annotated mucinous histology using a mucin gene-based ssGSEA score. Differential expression analysis was then performed to identify genes associated with mucinous histology, followed by GOEA, POEA, and DOEA to characterise biological pathways and drug-perturbation signatures. Finally, PPI analyses were performed to explore interactions between mucin genes and signalling molecules enriched in mucinous CRC.

RESULTS

A total of 984/991 cases had data for CRC histology, of which 15.7% (154/984) were mucinous adenocarcinoma and 84.3% (830/984) were non-mucinous adenocarcinoma. Validation of the annotated histological classification using mucin-related transcriptional signatures demonstrated that mucinous carcinoma exhibited significantly higher secreted mucin signature scores than non-mucinous adenocarcinoma (Mann–Whitney U test, standardized test statistic = −6.451, $P < 0.001$). In contrast, membranous mucin signature scores did not differ significantly between groups (standardized test statistic = −1.191, $P = 0.234$). When combined into a composite mucin signature, mucinous carcinoma again demonstrated significantly higher scores (standardized test statistic = −5.606, $P < 0.001$), supporting the validity of the annotated histological classification (Figure 1).

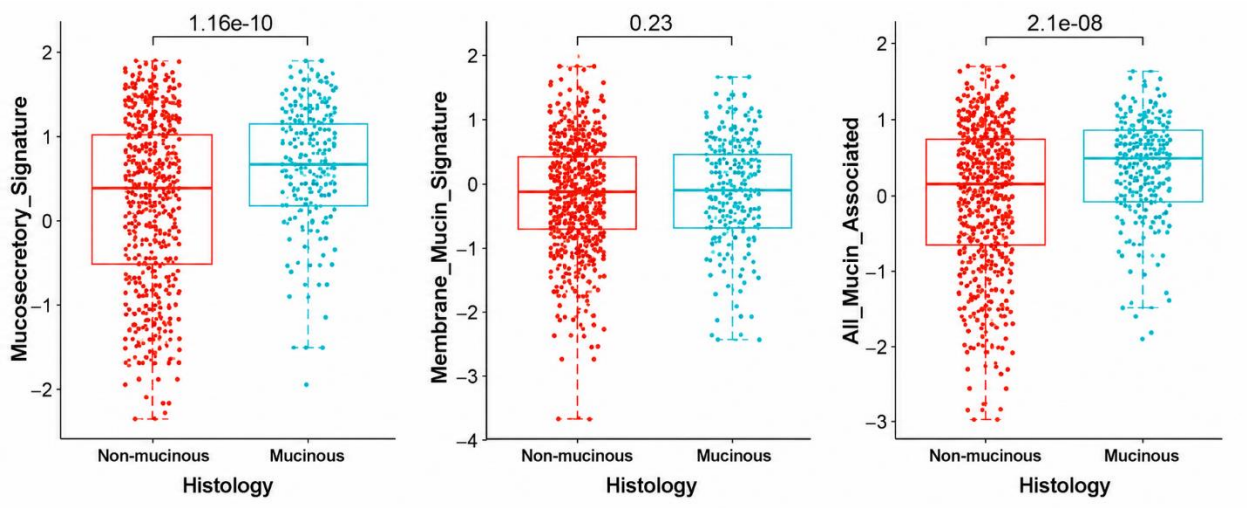

Figure 1: Validation of Histological Annotation Using Mucin-Related Transcriptional Signatures

Box-and-whisker plots with overlaid individual samples comparing secreted mucin, membranous mucin, and composite mucin transcriptional signature scores between histologically annotated mucinous and non-mucinous colorectal adenocarcinomas. Signature scores were generated by single-sample gene set enrichment analysis (ssGSEA) using predefined mucin gene sets. Boxes represent the interquartile range with the median, whiskers indicate 1.5× the interquartile range, and each point represents an individual tumour. P values were calculated using the Mann–Whitney U test. The concordance between transcriptional mucin signatures and the annotated histological groups provides biological validation of the histological classification.

Mucinous carcinoma displays differential clinicopathological and molecular correlates

Chi-square testing demonstrated that the mucinous histotype was associated with female gender, young age at presentation (< 50 years), late pathological tumour stage, and right-sided tumour location. No association was found with pathological node stage, metastasis stage, or overall TNM stage. Mucinous histology was associated with microsatellite instability (MSI), *BRAF* mutation positivity, *TP53* mutation negativity, low Fraction Genome Altered and Aneuploidy scores, and high Tumour Mutation Burden (Supplementary Materials 1; Figure 2). Binary logistic regression (Omnibus $\chi^2 = 74.997$, df = 4, $P < 0.001$) demonstrated that *BRAF* mutation ($P < 0.001$), *TP53* mutation ($P < 0.001$), and tumour location ($P = 0.037$) remained independently associated with mucinous histology, whereas MSI status was not ($P = 0.942$) (Table 1). Kaplan–Meier analysis demonstrated no association of mucinous histology with overall or disease-free survival (Log Rank: OS $\chi^2 = 0.409$, $P = 0.523$; DFS $\chi^2 = 0.022$, $P = 0.883$).

Table 1: Regression Analyses for The Mucinous Histology Associations

Features	Regression coefficient (B)	Standard Error of Regression	P value	Odds Ratio of Regression
BRAF mutation	-1.255	0.257	<0.001	0.285
MSI Status	0.092	0.311	0.767	1.097
Tumour Location	0.603	0.234	0.01	1.827
TMB	-0.204	0.486	0.675	0.816
Constant	1.745	0.482	<0.001	5.727

Cox & Snell R^2 = 0.075; Nagelkerke R^2 =0.126; Hosmer–Lemeshow goodness-of-fit test indicated good model calibration (χ^2 = 0.678, df = 5, P = 0.984)

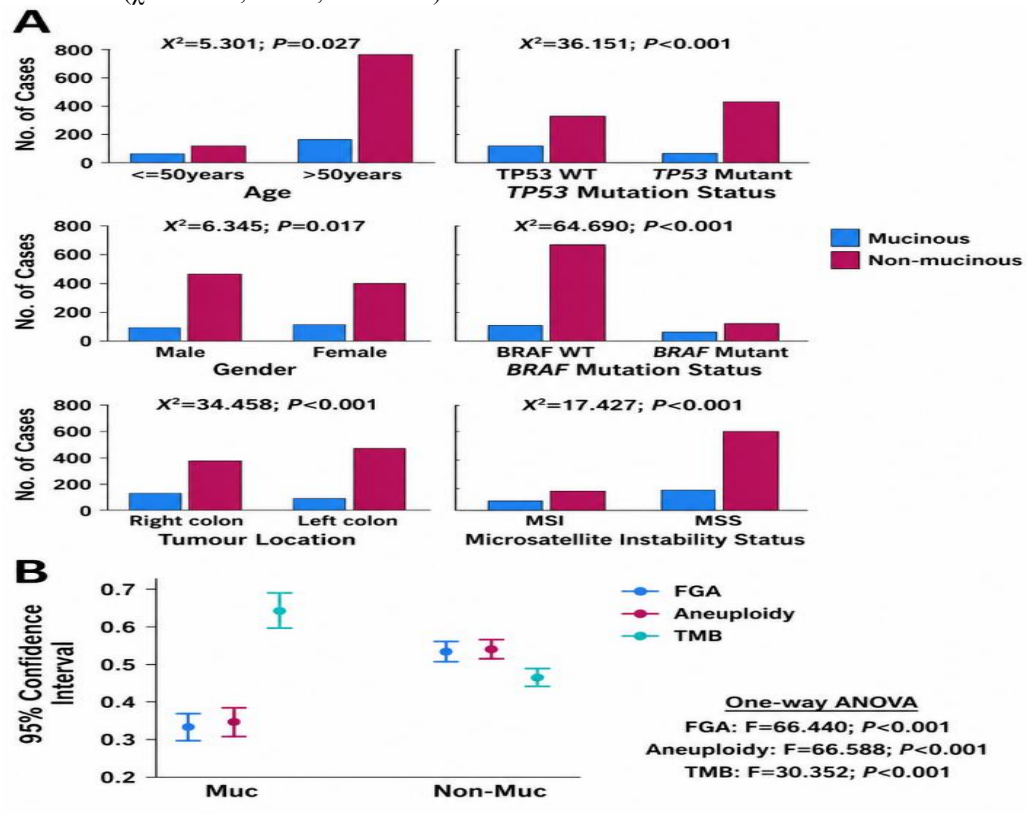

Figure 2: A. Clustered bar charts showing significant associations between mucinous carcinoma and the clinicopathological and molecular features of CRC, thereby confirming the finding from previous studies **B.** Error bars showing correlation of mucinous histology with genomic features of CRC, in keeping with the known biology of mucinous histological types of CRC.
Muc= mucinous adenocarcinoma (n=154), Non-Muc= non-mucinous adenocarcinoma (n=830)

Differential gene expression analysis of mucinous and non-mucinous colorectal carcinomas

DE analysis identified extensive transcriptional differences between mucinous and non-mucinous colorectal carcinomas (Supplementary Materials 2). The mucinous phenotype was characterised by marked upregulation of genes associated with mucin production, goblet cell differentiation, and secretory function. The most highly upregulated genes in mucinous carcinomas included *REG4* ($\log_2$FC = 1.53, adjusted $P = 7.80\times10^{-13}$), *MUC2* ($\log_2$FC = 1.44, adjusted $P = 6.19\times10^{-15}$), *SPINK4* ($\log_2$FC = 1.15, adjusted $P = 4.65\times10^{-8}$), *FCGBP* ($\log_2$FC = 1.00, adjusted $P = 2.87\times10^{-9}$), and *REG1A* ($\log_2$FC = 0.99, adjusted $P = 3.81\times10^{-5}$). Other prominently overexpressed genes included *SPDEF, TFF1, TFF2, AGR2, AGR3, CTSE, B3GNT6, GCNT3, ST6GALNAC1, CLCA1, ATOH1*, and *ERN2* (all adjusted $P < 0.05$). Overexpression of genes involved in mucin glycosylation (*B3GNT6, GCNT3, ST6GALNAC1*), secretory trafficking (*RAB26, RAB27B, XBP1*), inflammatory signalling (*IL1B, IL1R2, CXCL5*), and hypoxia (*CA9, EGLN3*) supported the secretory, inflammatory, and hypoxic microenvironment characteristic of mucinous CRC. In contrast, non-mucinous carcinomas preferentially overexpressed genes associated with epithelial differentiation, proliferative signalling, and metabolic homeostasis. Among the most significantly upregulated genes were *LY6G6D* ($\log_2$FC = −1.23, adjusted $P = 1.52\times10^{-12}$), *CEL* ($\log_2$FC = −1.03, adjusted $P = 7.58\times10^{-12}$), *ASCL2* ($\log_2$FC = −0.89, adjusted $P = 1.38\times10^{-13}$), *QPRT* ($\log_2$FC = −0.84, adjusted $P = 2.91\times10^{-13}$), and *SLC26A3* ($\log_2$FC = −0.80, adjusted $P = 8.40\times10^{-6}$). Additional highly expressed genes included *MYC, AXIN2, RNF43, NKD1, NKD2, HNF4A, POFUT1, FGFR4, AREG, EREG*, and *WNT11* (all adjusted $P < 0.05$), indicative of enhanced WNT/β-catenin and proliferative signalling.

Gene set enrichment analysis of mucinous and non-mucinous colorectal carcinomas

GSEA using the Hallmark gene set collection demonstrated profound transcriptional differences between mucinous and non-mucinous carcinomas (Supplementary Materials 3). Mucinous carcinomas were predominantly enriched for inflammatory, stromal, and microenvironment-associated programmes, whereas non-mucinous carcinomas exhibited enrichment of proliferative and metabolic pathways. The most significantly enriched Hallmark gene sets in mucinous carcinomas were Inflammatory Response (NES = 2.70, FDR < 0.001), Epithelial-Mesenchymal Transition (NES = 2.59, FDR < 0.001), TNFα Signalling via NFκB (NES = 2.56, FDR < 0.001), Hypoxia

(NES = 2.23, FDR < 0.001), and Complement (NES = 2.04, FDR < 0.001). Additional significantly enriched pathways included KRAS Signalling Up, IL6/JAK/STAT3 Signalling, Interferon Gamma Response, Allograft Rejection, Coagulation, Angiogenesis, IL2/STAT5 Signalling, Apoptosis, Glycolysis, Apical Junction, and Protein Secretion (all FDR < 0.05). In contrast, non-mucinous carcinomas demonstrated preferential enrichment of MYC Targets V2 (NES = −2.27, FDR < 0.001), MYC Targets V1 (NES = −2.15, FDR < 0.001), E2F Targets

(NES = −1.89, FDR < 0.001), Oxidative Phosphorylation (NES = −1.62, FDR = 0.013), Bile Acid Metabolism (NES = −1.54, FDR = 0.021), WNT/β-catenin Signalling (NES = −1.51, FDR = 0.022), and DNA Repair (NES = −1.50, FDR = 0.020) (Supplementary Materials 3).

Gene ontology and pathway enrichment analyses of mucinous and non-mucinous colorectal carcinomas

GOEA and POEA revealed marked biological divergence between mucinous and non-mucinous carcinomas. Within the GOBP 2026 library, the five most significantly enriched biological processes in mucinous carcinomas were Regulation of Cell Migration (112/484 genes; adjusted $P = 6.11\times10^{-19}$), Inflammatory Response (82/298 genes; adjusted $P = 1.72\times10^{-18}$), Extracellular Matrix Organization (63/192 genes; adjusted $P = 3.11\times10^{-18}$), Regulation of Angiogenesis (61/213 genes; adjusted $P = 1.93\times10^{-14}$), and Positive Regulation of Cell Motility (66/254 genes; adjusted $P = 1.70\times10^{-13}$). Additional enriched processes included collagen fibril organization, endothelial cell proliferation, vasculature development, and inflammatory signalling pathways (Supplementary Materials 4). In contrast, non-mucinous carcinomas demonstrated enrichment of Ribosome Biogenesis (58/171 genes; adjusted $P = 4.88\times10^{-15}$), Translation (72/251 genes; adjusted $P = 7.37\times10^{-15}$), rRNA Processing (47/137 genes; adjusted $P = 1.87\times10^{-12}$), Cytoplasmic Translation (39/106 genes; adjusted $P = 2.67\times10^{-11}$), and Protein Biosynthetic Process (46/147 genes; adjusted $P = 1.08\times10^{-10}$) (Supplementary Materials 4). POEA using the Panther 2016 library further underscored these differences. In mucinous carcinomas, the five most significantly enriched pathways were Integrin Signalling (51/156 genes; adjusted $P = 1.55\times10^{-15}$), Inflammation Mediated by Chemokine and Cytokine Signalling (47/188 genes; adjusted $P = 8.53\times10^{-10}$), Angiogenesis (29/142 genes; adjusted $P = 3.37\times10^{-4}$), CCKR Signalling (31/165 genes; adjusted $P = 7.27\times10^{-4}$), and Plasminogen Activating Cascade (7/15 genes; adjusted $P = 0.0024$). Additional enriched pathways included apoptosis, p53, PDGF, JAK/STAT, T-cell activation, VEGF, and interleukin signalling (Supplementary Materials 5). No Panther pathway reached statistical significance in the non-mucinous group following multiple-testing correction.

Mucinous carcinoma-specific signalling pathways exhibit interactions with mucin genes

To investigate whether mucin-associated proteins are functionally incorporated into signalling pathways enriched in mucinous CRC, pathway-specific PPI networks were constructed by combining genes from each significantly enriched pathway with a predefined mucin-associated gene set (*MUC2, MUC5AC, MUC6, FCGBP, AGR2, AGR3, SPINK4* and *CLCA1*). STRING analysis demonstrated significantly greater protein–protein interactions than expected for a random protein set of equivalent size (PPI enrichment P < 0.001), indicating that the analysed proteins are functionally connected rather than randomly associated. Networks were generated using STRING (minimum interaction score ≥ 0.400) and analysed in Cytoscape using NetworkAnalyzer and MCODE (Table 2, Supplementary Materials

6). The Inflammation/Chemokine pathway demonstrated extensive incorporation of the mucosecretory programme. MCODE identified a mixed module containing *KRAS, PTGS2, CXCR2* and *GNAQ* together with *MUC2, AGR2, FCGBP, SPINK4* and *CLCA1*. Similarly, the TLR pathway demonstrated substantial integration, with a mixed module comprising *TLR2, TLR4* and *PTGS2* together with the same mucin-associated proteins. The T-cell activation pathway likewise contained a mixed module consisting of *PTPRC, CD74, CD86, HLA-DRA* and *LCP2* together with *MUC2, AGR2, FCGBP, SPINK4* and *CLCA1*. The p53 feedback-loop pathway exhibited the greatest degree of mucin integration, with six mucin-associated genes (*AGR2, MUC5AC, MUC6, FCGBP, SPINK4* and *CLCA1*) co-clustering with *TP53, KRAS, PTEN, MDM2, CDKN1A, PIK3CD, PIK3R3, PIK3R5, AKT3* and *PPP2CB*. The CCKR pathway demonstrated moderate integration, with a mixed module comprising *MUC2, MUC6, AGR2, TFF1* and *TFF2*. Furthermore, the PDGF signalling pathway exhibited the least degree of mucin integration, with a single PDGF signalling pathway gene (*SPDEF*) co-clustering with *MUC2, MUC5AC, SPINK4, AGR2, FBCGP*, and *CLCA1* (Supplementary Materials 6). In contrast, the other seven pathways enriched in the mucinous carcinoma subset demonstrated no integration, exhibiting separate mucosecretory module and the specific pathway modules. Collectively, these analyses demonstrate that mucin-associated proteins are selectively incorporated into inflammatory, innate immune, adaptive immune and p53-associated signalling networks, while remaining largely segregated from structural extracellular matrix and growth factor signalling pathways (Figure 3).

Table 2: Integration of Mucin Genes into Enriched Pathway Protein–Protein Interaction Networks and Their Associated Bridge Genes

Pathway Network	**Mucin Genes in Pathway Clusters**	**Key Bridge Gene(s)**
Inflammation/Chemokine signalling	MUC2, AGR2, CLCA1, FCGBP, SPINK4	KRAS, PTGS2, CXCR2, GNAQ
PDGF signalling	MUC2, AGR2, CLCA1, SPINK4, FCGBP, MUC5AC	SPDEF
T-cell Activation	MUC2, AGR2, CLCA1, SPINK4, FCGBP	CD86, CD74, LCP2, PTPRC, HLA-DRA
TLR signalling	MUC2, AGR2, CLCA1, SPINK4, FCGBP	TLR2, TLR4, PTGS2
p53 feedback loops 2	AGR2, CLCA1, SPINK4, FCGBP, MUC5AC, MUC6	KRAS, TP53, MDM2, PTEN, AKT3
CCKR signalling map	AGR2, MUC2, MUC6	TFF1, TFF2
Angiogenesis	None	N/A
VEGF signalling	None	N/A
Plasminogen activation cascade	None	N/A
Apoptosis signalling	None	N/A
JAK-STAT signalling	None	N/A
Interleukin signaling	None	N/A
p53 pathway	None	N/A
Pyrimidine Metabolism	None	N/A
5-HT degradation	None	N/A

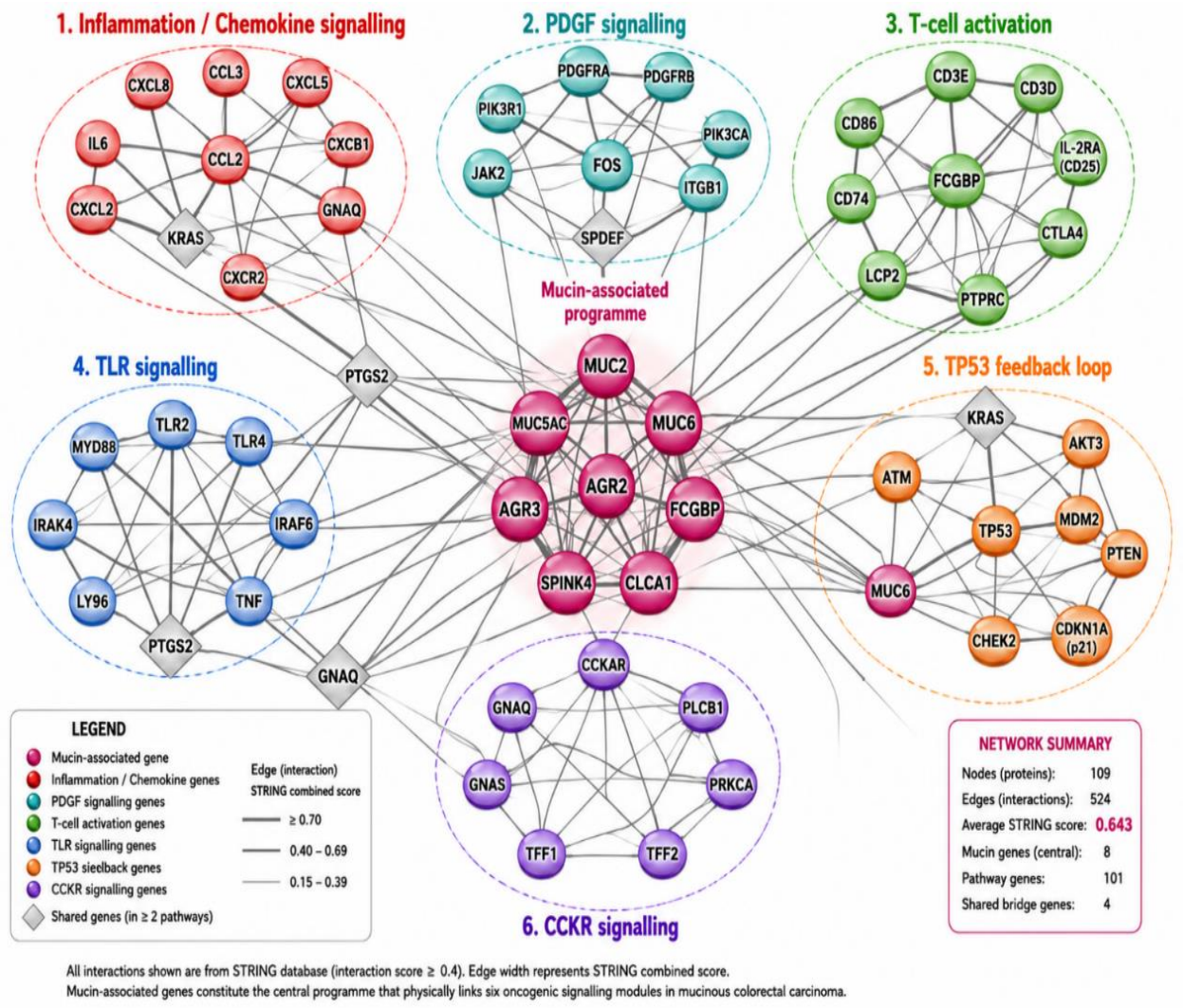

Figure 3: Integrated Protein–Protein Interaction Network Linking the Mucin Programme to Enriched Signalling Pathways in Mucinous Colorectal Carcinoma

The central mucin-associated programme comprises secreted and mucin-associated proteins (*MUC2, MUC5AC, MUC6, AGR2, AGR3, FCGBP, SPINK4* and *CLCA1*), which are connected to six signalling modules identified by Reactome pathway enrichment and STRING protein–protein interaction analysis: (1) inflammation/chemokine signalling, (2) PDGF signalling, (3) T-cell activation, (4) Toll-like receptor (TLR) signalling, (5) TP53 feedback loop, and (6) CCKR signalling. Pathway genes are colour-coded according to their respective signalling modules, whereas mucin-associated genes are shown in magenta. Grey diamond-shaped nodes denote bridge proteins shared between two or more pathway modules. Edges represent STRING protein–protein interactions with a combined confidence score ≥0.400, with thicker lines indicating higher interaction confidence. The integrated network demonstrates that the mucin programme occupies a central position linking multiple oncogenic, inflammatory and immune-related signalling pathways

through shared interaction hubs, supporting coordinated pathway cross-talk in mucinous colorectal carcinoma. The complete network comprises 109 proteins connected by 524 unique protein–protein interactions, with an average STRING combined interaction score of 0.643.

Drug ontology enrichment identifies transcriptional associations with SMI response signatures

DOEA using the enriched genes from DE analyses demonstrated preferential enrichment of responses to calcium channel blockers (CCBs), mucolytic drugs and *N*-glycosylation inhibitors in the mucinous subset (Supplementary Materials 7).

Mucinous carcinoma exhibits enrichment of mucolytic drug responses

DOEF and DOOR analysess of mucolytic drug perturbation signatures revealed significant preferential enrichment in mucinous CRC for guaifenesin and telmesteine (Table 3, Figure 4A, Supplementary Materials 7). Although bromhexine and ambroxol also exhibited higher enrichment statistics in the mucinous subset, these differences did not reach statistical significance.

Preferential enrichment of calcium-channel blocker responses

DOEF and DOOR analyses consistently demonstrated preferential enrichment of CCB perturbation signatures in mucinous CRC (Table 4, Figure 4B). Significant enrichment was observed for amlodipine, benidipine, budipine, felodipine, isradipine, lacidipine, nicardipine, nifedipine, nilvadipine, nimodipine, nisoldipine, nitrendipine, pranidipine, riodipine, diltiazem, and verapamil (Table 4, Supplementary Materials 7). No CCB signature demonstrated preferential enrichment in the non-mucinous subset.

Table 3: Differential Enrichment of Mucolytic Drug-Response Signatures in Mucinous Versus Non-Mucinous Colorectal Carcinoma

Drug signature	DOEF z	DOEF P	DOOR z	DOOR P	Interpretation
Guaifenesin	5.013	5.37×10^{-7}	4.743	2.11×10^{-6}	Mucinous
Telmesteine	2.275	2.29×10^{-2}	2.275	2.29×10^{-2}	Mucinous
Bromhexine	1.761	7.83×10^{-2}	1.77	7.67×10^{-2}	NS
Ambroxol	1.341	1.80×10^{-1}	1.354	1.76×10^{-1}	NS

Enrichment of *N*-glycosylation inhibitor and bosutinib responses

Perturbation signatures associated with inhibition of *N*-linked glycosylation were preferentially enriched in the mucinous subset, with significant enrichment observed for acarbose, castanospermine, kifunensine, swainsonine, and brefeldin A (Table 5, Figure 4A, Supplementary Materials 7). In addition, the Src/Abl tyrosine kinase inhibitor bosutinib demonstrated significant preferential enrichment in mucinous carcinoma.

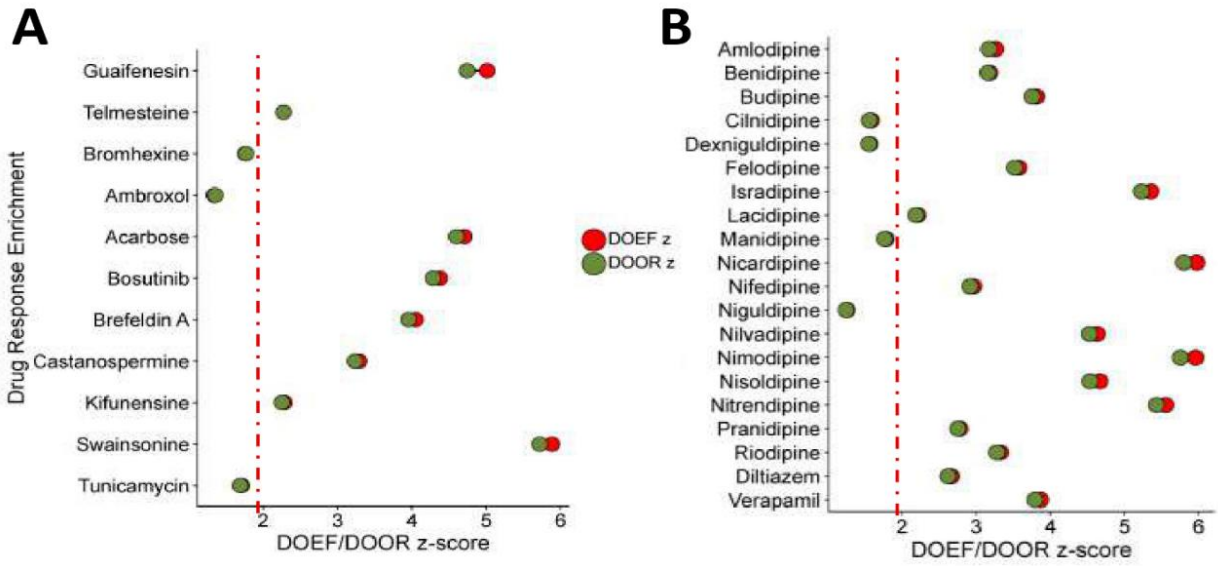

Figure 4: Drug Signature Enrichment Analyses Identify Preferential Responses to Mucolytic Agents, Calcium-Channel Blockers, And N-Glycosylation Inhibitors In Mucinous Colorectal Carcinoma. (A) DOEF and DOOR analyses of LINCS 1000 Chem Perturb drug signatures for mucolytic agents and N-glycosylation inhibitors/Bosutinib. (B) DOEF and DOOR analyses of calcium-channel blocker drug signatures.

For each drug, red and green circles represent the enrichment z-scores obtained by the Differential Ontology Enrichment Fraction (DOEF) and Differential Ontology Odd Ratio (DOOR), respectively. The vertical dashed line indicates the nominal significance threshold ($z = 1.96$; $P = 0.05$), with points to the right representing significantly enriched drug-response signatures in the mucinous compared to the non-mucinous carcinoma subsets. The close correspondence between DOEF and DOOR z-scores demonstrates the high concordance of the two analytical approaches across all evaluated drug signatures.

Table 4: Differential Enrichment of Calcium Channel Blockers-Response Signatures in Mucinous Versus Non-Mucinous Colorectal Carcinoma.

Drug signature	DOEF z	DOEF P	DOOR z	DOOR P	Interpretation
Amlodipine	3.263	1.10×10^{-3}	3.171	1.52×10^{-3}	Mucinous
Benidipine	3.181	1.47×10^{-3}	3.157	1.59×10^{-3}	Mucinous
Budipine	3.812	1.38×10^{-4}	3.756	1.73×10^{-4}	Mucinous
Cilnidipine	1.586	1.13×10^{-1}	1.561	1.19×10^{-1}	NS
Dexniguldipine	1.566	1.17×10^{-1}	1.554	1.20×10^{-1}	NS
Felodipine	3.575	3.50×10^{-4}	3.518	4.34×10^{-4}	Mucinous
Isradipine	5.353	8.67×10^{-8}	5.228	1.71×10^{-7}	Mucinous
Lacidipine	2.211	2.70×10^{-2}	2.187	2.87×10^{-2}	Mucinous
Manidipine	1.787	7.40×10^{-2}	1.767	7.73×10^{-2}	NS
Nicardipine	5.972	2.35×10^{-9}	5.799	6.69×10^{-9}	Mucinous
Nifedipine	2.962	3.06×10^{-3}	2.917	3.53×10^{-3}	Mucinous
Niguldipine	1.261	2.07×10^{-1}	1.247	2.12×10^{-1}	NS
Nilvadipine	4.629	3.67×10^{-6}	4.527	5.98×10^{-6}	Mucinous
Nimodipine	5.958	2.56×10^{-9}	5.755	8.68×10^{-9}	Mucinous
Nisoldipine	4.666	3.07×10^{-6}	4.535	5.77×10^{-6}	Mucinous
Nitrendipine	5.556	2.76×10^{-8}	5.431	5.60×10^{-8}	Mucinous
Pranidipine	2.783	5.39×10^{-3}	2.755	5.86×10^{-3}	Mucinous
Riodipine	3.324	8.87×10^{-4}	3.279	1.04×10^{-3}	Mucinous
Diltiazem	2.663	7.75×10^{-3}	2.623	8.72×10^{-3}	Mucinous
Verapamil	3.869	1.09×10^{-4}	3.796	1.47×10^{-4}	Mucinous

Table 5: Differential Enrichment Of N-Linked Glycosylation Inhibitor-Response Signatures in Mucinous Versus Non-Mucinous Colorectal Carcinoma.

Drug signature	DOEF z	DOEF P	DOOR z	DOOR P	Interpretation
Acarbose	4.707	2.51×10^{-6}	4.6	4.23×10^{-6}	Mucinous
Bosutinib	4.378	1.20×10^{-5}	4.283	1.85×10^{-5}	Mucinous
Brefeldin A	4.052	5.08×10^{-5}	3.955	7.66×10^{-5}	Mucinous
Castanospermine	3.291	9.98×10^{-4}	3.236	1.21×10^{-3}	Mucinous
Kifunensine	2.285	2.23×10^{-2}	2.252	2.43×10^{-2}	Mucinous
Swainsonine	5.885	3.99×10^{-9}	5.722	1.05×10^{-8}	Mucinous
Tunicamycin	1.709	8.74×10^{-2}	1.692	9.06×10^{-2}	NS

DISUSSION

The present study provides a comprehensive transcriptomic characterization of mucinous

colorectal carcinoma using three integrated CRC cohorts and confirms that mucinous histology represents a biologically distinct tumour phenotype. Consistent with previous reports, mucinous carcinomas were associated with younger age, female sex, right-sided tumour location, microsatellite instability (MSI), *BRAF* mutation, high tumour mutational burden, and reduced chromosomal instability.[5–7,34–39] Logistic regression further demonstrated that the association between mucinous histology and *BRAF* mutation was independent of tumour location (Table 1), consistent with previous observations.[34,35] In contrast, mucinous histology was not associated with overall or disease-free survival, highlighting the biological heterogeneity of this tumour subtype. Although several studies have reported poorer outcomes in mucinous CRC, prognostic differences are strongly influenced by tumour stage, MSI status, tumour location, and accompanying molecular alterations.[5–7,35–39] Consequently, the absence of survival differences in the present study likely reflects the molecular diversity of the integrated cohorts rather than contradicting the existing literature.

An important strength of this study was the biological validation of the annotated histological classification before downstream analyses. The significantly higher secreted mucin and composite mucin signature scores observed in annotated mucinous carcinomas confirmed that the pathological classifications reflected genuine biological differences rather than arbitrary clinical annotations. This validation was particularly important because the transcriptomic data were obtained from multiple public cohorts in which central pathology review was not feasible. Histopathological assessment of mucinous differentiation is known to exhibit interobserver variability, and application of the World Health Organization criterion requiring extracellular mucin to comprise more than 50% of tumour volume may vary across institutions. Nevertheless, the observed prevalence of mucinous carcinoma (15.7%) lies within the widely reported range of 10–25%, supporting the overall validity of the histological annotations used in this study.[5-7]

Beyond confirming established clinicopathological associations, the integrated transcriptomic analyses demonstrated that mucinous CRC possesses a distinctive tumour microenvironment characterized by inflammatory, stromal, hypoxic, angiogenic and extracellular matrix-associated biological programmes. GSEA showed preferential enrichment of inflammatory response, epithelial–mesenchymal transition, TNFα/NFκB signalling, hypoxia, complement activation and cytokine signalling, whereas non-mucinous carcinomas preferentially exhibited proliferative, metabolic and MYC-driven programmes. These observations agree with the recognized role of the tumour microenvironment as an active regulator of tumour progression, immune modulation, invasion and therapeutic resistance rather than merely a structural scaffold.[40-44] The GOEA and POEA findings further reinforced this concept by demonstrating enrichment of pathways regulating cell migration, extracellular matrix organization, angiogenesis, inflammatory signalling and immune responses specifically within mucinous carcinomas.

Protein–protein interaction analyses extended these observations by demonstrating that mucin-associated genes were selectively incorporated into inflammatory, innate immune, adaptive immune and p53-associated signalling networks, while remaining largely segregated from structural extracellular matrix and PDGF signalling pathways. Rather than functioning as signalling hubs, *AGR2 and MUC2* emerged as the most recurrent mucin-associated genes across pathway-specific interaction networks (Figure 3; Supplementary Materials 6), suggesting that the mucosecretory programme is closely integrated with inflammatory and stress-response pathways within the mucinous tumour microenvironment. These findings support the concept that mucinous histology reflects coordinated remodelling of multiple biological processes rather than isolated overproduction of extracellular mucin and provide a mechanistic framework for understanding the distinctive biology of this colorectal cancer subtype.[40-44]

An important objective of this study was to determine whether mucinous colorectal carcinoma exhibits preferential transcriptional associations with drug-perturbation signatures related to anti-mucin therapeutic strategies. DOEA consistently demonstrated preferential enrichment of calcium channel blocker (CCB), mucolytic, N-glycosylation inhibitor (NLGi), and Bosutinib signatures in the mucinous subset. These findings should be interpreted as transcriptional associations derived from the LINCS L1000 perturbation database rather than evidence of therapeutic efficacy, and therefore provide hypotheses for future experimental investigation rather than immediate clinical application.

The enrichment of CCB signatures is biologically plausible given the established role of calcium signalling in mucin secretion. Cantero-Recasens et al. demonstrated that Na^+/Ca^{2+} exchanger 2 (NCX2) cooperates with TRPM4 to regulate calcium-dependent secretion of MUC2 and MUC5AC, while pharmacological inhibition reduced mucin secretion from goblet cells.[15,16] More recently, selective inhibition of NCX with SN-6 restored chemosensitivity in mucin-producing colorectal cancer organoids, supporting the concept that disruption of calcium-dependent mucin secretion may enhance therapeutic response.[45] Although the present study did not directly investigate NCX2 or SN-6, the enrichment of CCB-associated signatures is consistent with these experimental observations. Furthermore, TRPM4 has recently been associated with tumour budding, invasion and adverse prognosis in colorectal cancer,[46,47] suggesting that calcium-regulated mucin secretion may contribute to the aggressive biology of mucinous CRC.

Preferential enrichment of NLGi signatures is likewise consistent with the essential role of N-linked glycosylation in mucin maturation and secretion.[12–14,48–56] Although currently available glycosylation inhibitors are limited by toxicity,[57] their enrichment suggests that mucin glycosylation pathways may represent exploitable biological vulnerabilities. Similarly, Bosutinib enrichment agrees with experimental evidence that Src inhibition suppresses MUC1 and MUC5AC expression through the Src–ERK/AKT–FOSL1 pathway,[11] although validation in colorectal cancer remains necessary.

The independent association between mucinous histology and *BRAF* mutation also provides important therapeutic context. Encorafenib combined with cetuximab is now an established treatment for metastatic *BRAF* V600E-mutant colorectal cancer,[58] highlighting the importance of molecular stratification. In addition, recent identification of L1TD1 as a regulator of mucinous adenocarcinoma biology[59] supports the concept that mucinous carcinoma possesses distinctive transcriptional programmes beyond excessive mucin production.

The drug ontology findings should nevertheless be interpreted cautiously. LINCS L1000 signatures are derived from transcriptional responses of cultured cell lines and do not establish target engagement, drug sensitivity, or clinical efficacy.60 Consequently, the enriched drug signatures identified here should be regarded as candidate therapeutic hypotheses requiring validation in mucinous CRC cell lines, organoids, and patient-derived xenograft models before translational conclusions can be drawn.

This study has several strengths. To our knowledge, it is one of the largest integrated transcriptomic investigations of mucinous colorectal carcinoma and among the first to combine differential expression, gene set enrichment, ontology enrichment, pathway-specific protein–protein interaction, DOEF, and DOOR analyses to characterize its biological and therapeutic landscape. Integration of three independent CRC cohorts, ComBat batch correction, and biological validation of annotated mucinous histology using mucin gene-expression signatures further strengthened the robustness of the findings.

Several limitations should be acknowledged. First, this retrospective study of publicly available datasets should be regarded as hypothesis-generating. Second, histological classification relied on study annotations without central pathology review. Although mucinous histology was biologically validated by higher secreted mucin signature scores and its prevalence was consistent with published epidemiological data, interinstitutional variation in pathological assessment may have resulted in some histological misclassification. Third, bulk RNA sequencing cannot distinguish tumour-cell-specific transcription from stromal, immune, and other tumour microenvironment components. Fourth, LINCS L1000 perturbation signatures reflect transcriptional responses to drug exposure rather than direct measures of drug sensitivity or clinical efficacy; therefore, the enriched signatures represent candidate biological associations rather than evidence of therapeutic effectiveness. Finally, although pathway-specific protein interaction analyses demonstrated selective incorporation of mucin-associated proteins into inflammatory and stress-response signalling networks, these computational findings require experimental validation.

Future studies should validate these findings in independent cohorts with central pathology review and investigate the identified candidate anti-mucin strategies using colorectal cancer cell lines, patient-derived organoids, and xenograft models. Functional studies of calcium-dependent mucin secretion, mucin glycosylation, and pathway-specific signalling interactions are needed to determine whether

the identified transcriptional associations translate into therapeutic vulnerabilities. Integration of single-cell and spatial transcriptomics may further define the cellular basis of mucin-associated signalling and support biomarker-guided, multitargeted therapies for mucinous colorectal carcinoma.

CONCLUSION

This integrated multi-cohort transcriptomic study demonstrates that mucinous colorectal carcinoma possesses a distinct inflammatory, immune, stromal and mucosecretory tumour microenvironment. Pathway-specific protein interaction analyses further revealed selective integration of mucin-associated proteins into inflammatory and stress-response signalling networks. Differential drug ontology enrichment identified transcriptional associations with calcium channel blockers, mucolytics, N-glycosylation inhibitors and Bosutinib, generating candidate anti-mucin therapeutic hypotheses. These findings provide a framework for future mechanistic and translational studies aimed at improving the management of mucinous colorectal carcinoma.

Declarations

Funding: No funding was received for this study

Institutional Review Board Statement: Not applicable.

Informed Consent Statement: Not applicable.

Data Availability Statement: All the data explored in this study are domiciled in the Genome Data Commons (https://portal.gdc.cancer.gov/) and the cBioPortal for Cancer Genomics (https://www.cbioportal.org/) databases.

Acknowledgments: The authors wish to express their sincere gratitude to the Genome Data Commons and the cBioPortal for Cancer Genomics for making the cancer genomics data freely available.

Conflicts of Interest: The authors declare no conflicts of interest.

REFERENCES

1. Bray F, Laversanne M, Sung H, et al. Global cancer statistics 2022: GLOBOCAN estimates of incidence and mortality worldwide for 36 cancers in 185 countries. CA Cancer J Clin. 2024;74:229-263. doi:10.3322/caac.21834
2. Filho AM, Laversanne M, Ferlay J, et al. The GLOBOCAN 2022 cancer estimates: data sources, methods, and a snapshot of the cancer burden worldwide. Int J Cancer. 2025;156:1336-1346. doi:10.1002/ijc.35278
3. Sung H, Ferlay J, Siegel RL, et al. Global cancer statistics 2020: GLOBOCAN estimates of incidence and mortality worldwide for 36 cancers in 185 countries. CA Cancer J Clin. 2021;71:209-249. doi:10.3322/caac.21660
4. Keum N, Giovannucci E. Global burden of colorectal cancer: emerging trends, risk factors and prevention strategies. Nat Rev Gastroenterol Hepatol. 2019;16:713-732. doi:10.1038/s41575-019-0189-8
5. Luo C, Cen S, Ding G, et al. Mucinous colorectal adenocarcinoma: clinical pathology and treatment options. Cancer Commun (Lond). 2019;39:13. doi:10.1186/s40880-019-0361-0
6. Verhulst J, Ferdinande L, Demetter P, et al. Mucinous subtype as prognostic factor in colorectal cancer: a systematic review and

meta-analysis. J Clin Pathol. 2012;65:381-388. doi:10.1136/jclinpath-2011-200340
7. Wang X, Wang H, He H, et al. Clinicopathological and prognostic features of colorectal mucinous adenocarcinomas: a systematic review and meta-analysis. BMC Cancer. 2024;24:1161. doi:10.1186/s12885-024-12905-3
8. Gautam SK, Kumar S, Cannon A, et al. MUC4 mucin- a therapeutic target for pancreatic ductal adenocarcinoma. Expert Opin Ther Targets. 2017;21:657-669. doi:10.1080/14728222.2017.1323880
9. Hasegawa M, Sinha RK, Kumar M, et al. Intracellular targeting of the oncogenic MUC1-C protein with a novel GO-203 nanoparticle formulation. Clin Cancer Res. 2015;21:2338-2347. doi:10.1158/1078-0432.CCR-14-3000
10. Lee DH, Choi S, Park Y, et al. Mucin1 and Mucin16: therapeutic targets for cancer therapy. Pharmaceuticals (Basel). 2021;14:1053. doi:10.3390/ph14101053
11. Zhang C, Atri P, Nallasamy P, et al. Small molecule inhibitor against onco-mucins disrupts Src/FosL1 axis to enhance gemcitabine efficacy in pancreatic ductal adenocarcinoma. Cancer Lett. 2022;551:215922. doi:10.1016/j.canlet.2022.215922
12. Adler KB, Tuvim MJ, Dickey BF. Regulated mucin secretion from airway epithelial cells. Front Endocrinol (Lausanne). 2013;4:129. doi:10.3389/fendo.2013.00129
13. Holmén Larsson JM, Thomsson KA, Rodríguez-Piñeiro AM, et al. Studies of mucus in mouse stomach, small intestine, and colon. III. Gastrointestinal Muc5ac and Muc2 mucin O-glycan patterns reveal a regiospecific distribution. Am J Physiol Gastrointest Liver Physiol. 2013;305:G357-G363. doi:10.1152/ajpgi.00048.2013
14. Thornton DJ, Rousseau K, McGuckin MA. Structure and function of the polymeric mucins in airways mucus. Annu Rev Physiol. 2008;70:459-486. doi:10.1146/annurev.physiol.70.113006.100702
15. Cantero-Recasens G, Butnaru CM, Brouwers N, et al. Sodium channel TRPM4 and sodium/calcium exchangers (NCX) cooperate in the control of Ca2+-induced mucin secretion from goblet cells. J Biol Chem. 2019;294:816-826. doi:10.1074/jbc.RA117.000848
16. Mitrovic S, Nogueira C, Cantero-Recasens G, et al. TRPM5-mediated calcium uptake regulates mucin secretion from human colon goblet cells. Elife. 2013;2:e00658. doi:10.7554/eLife.00658
17. Liu GH, Chen T, Zhang X, et al. Small molecule inhibitors targeting the cancers. MedComm. 2022;3:e181. doi:10.1002/mco2.181
18. Zhong S, Jeong JH, Chen Z, et al. Targeting tumor microenvironment by small-molecule inhibitors. Transl Oncol. 2020;13:57-69. doi:10.1016/j.tranon.2019.10.001
19. Liu J, Lichtenberg T, Hoadley KA, et al. An integrated TCGA pan-cancer clinical data resource to drive high-quality survival outcome analytics. Cell. 2018;173:400-416. doi:10.1016/j.cell.2018.02.052
20. Roelands J, Kuppen PJK, Ahmed EI, et al. An integrated tumor, immune and microbiome atlas of colon cancer. Nat Med. 2023;29:1273-1286. doi:10.1038/s41591-023-02324-5
21. Vasaikar S, Huang C, Wang X, et al. Proteogenomic analysis of human colon cancer reveals new therapeutic opportunities. Cell. 2019;177:1035-1049. doi:10.1016/j.cell.2019.03.030
22. Gao J, Aksoy BA, Dogrusoz U, et al. Integrative analysis of complex cancer genomics and clinical profiles using the cBioPortal. Sci Signal. 2013;6:pl1. doi:10.1126/scisignal.2004088
23. Cerami E, Gao J, Dogrusoz U, et al. The cBio cancer genomics portal: an open platform for exploring multidimensional cancer genomics

data. Cancer Discov. 2012;2:401-404. doi:10.1158/2159-8290.CD-12-0095
24. Johnson WE, Li C, Rabinovic A. Adjusting batch effects in microarray expression data using empirical Bayes methods. Biostatistics. 2007;8(1):118–127. doi:10.1093/biostatistics/kxj037.
25. Johansson MEV, Ambort D, Pelaseyed T, et al. Composition and functional role of the mucus layers in the intestine. Cell Mol Life Sci. 2011;68:3635–3641.
26. Hu FJ, Li YJ, Zhang L, Ji DB, et.al. Single-cell profiling reveals differences between human classical adenocarcinoma and mucinous adenocarcinoma. Commun Biol. 2023 Jan 23;6(1):85. doi: 10.1038/s42003-023-04441-w.
27. Gan G-L, Liu J, Chen W-J, Ye Q-Q, et.al. (2020) The Diverse Roles of the Mucin Gene Cluster Located on Chromosome 11p15.5 in Colorectal Cancer. Front. Cell Dev. Biol. 8:514. doi: 10.3389/fcell.2020.00514
28. Ritchie ME, Phipson B, Wu D, Hu Y, et.al. limma powers differential expression analyses for RNA-sequencing and microarray studies. Nucleic Acids Research. 2015;43(7):e47. doi:10.1093/nar/gkv007.
29. Maleki F, Ovens K, Hogan DJ, et al. Gene set analysis: challenges, opportunities, and future research. Front Genet. 2020;11:654. doi:10.3389/fgene.2020.00654
30. Xie Z, Bailey A, Kuleshov MV, et al. Gene set knowledge discovery with Enrichr. Curr Protoc. 2021;1:e90. doi:10.1002/cpz1.90
31. Kuleshov MV, Jones MR, Rouillard AD, Fernandez NF, et.al. Enrichr: a comprehensive gene set enrichment analysis web server 2016 update. Nucleic Acids Research. 2016;44(W1):W90–W97. doi:10.1093/nar/gkw377.
32. Szklarczyk D, Kirsch R, Koutrouli M, et al. The STRING database in 2023: protein-protein association networks and functional enrichment analyses for any sequenced genome of interest. Nucleic Acids Res. 2023;51:D638-D646. doi:10.1093/nar/gkac1000
33. Kohl M, Wiese S, Klein K. Cytoscape: software for visualization and analysis of biological networks. Methods Mol Biol. 2011;696:219-53.
34. Pai RK, Jayachandran P, Koong AC, et al. BRAF-mutated, microsatellite-stable adenocarcinoma of the proximal colon: an aggressive adenocarcinoma with poor survival, mucinous differentiation, and adverse morphologic features. Am J Surg Pathol. 2012;36:744-752. doi:10.1097/PAS.0b013e31824430d7
35. Jang MH, Kim S, Hwang DY, et al. BRAF-mutated colorectal cancer exhibits distinct clinicopathological features from wild-type BRAF-expressing cancer independent of the microsatellite instability status. J Korean Med Sci. 2017;32:38-46. doi:10.3346/jkms.2017.32.1.38
36. Phipps AI, Buchanan DD, Makar KW, et al. BRAF mutation status and survival after colorectal cancer diagnosis according to patient and tumor characteristics. Cancer Epidemiol Biomarkers Prev. 2012;21:1792-1798. doi:10.1158/1055-9965.EPI-12-0674
37. Bae JM, Kim JH, Kang GH. Molecular subtypes of colorectal cancer and their clinicopathologic features, with an emphasis on the serrated neoplasia pathway. Arch Pathol Lab Med. 2016;140:406-412. doi:10.5858/arpa.2015-0310-RA
38. Huang A, Yang Y, Shi JY, et al. Mucinous adenocarcinoma: a unique clinicopathological subtype in colorectal cancer. World J Gastrointest Surg. 2021;13:1567-1583. doi:10.4240/wjgs.v13.i12.1567
39. Phipps AI, Limburg PJ, Baron JA, et al. Association between molecular subtypes of colorectal cancer and patient survival. Gastroenterology. 2015;148:77-87. doi:10.1053/j.gastro.2014.09.038
40. Ho WJ, Jaffee EM, Zheng L. The tumour microenvironment in pancreatic cancer—

clinical challenges and opportunities. Nat Rev Clin Oncol. 2020;17:527-540. doi:10.1038/s41571-020-0363-5
41. Dvorak HF, Weaver VM, Tlsty TD, et al. Tumor microenvironment and progression. J Surg Oncol. 2011;103:468-474. doi:10.1002/jso.21709
42. Li Z, Yin P. Tumor microenvironment diversity and plasticity in cancer multidrug resistance. Biochim Biophys Acta Rev Cancer. 2023;1878:188997. doi:10.1016/j.bbcan.2023.188997
43. Li Q, Geng S, Luo H, et al. Signaling pathways involved in colorectal cancer: pathogenesis and targeted therapy. Signal Transduct Target Ther. 2024;9:266. doi:10.1038/s41392-024-01953-7
44. Moench R, Gasser M, Nawalaniec K, et al. Platelet-derived growth factor (PDGF) cross-signaling via non-corresponding receptors indicates bypassed signaling in colorectal cancer. Oncotarget. 2022;13:1140-1152. doi:10.18632/oncotarget.28281
45. Cantero-Recasens G, Alonso-Marañón J, Lobo-Jarne T, et.al. Reversing chemorefraction in colorectal cancer cells by controlling mucin secretion. Elife. 2022;11:e73926. doi: 10.7554/eLife.73926.
46. Kappel S, Stokłosa P, Hauert B, et.al. TRPM4 is highly expressed in human colorectal tumor buds and contributes to proliferation, cell cycle, and invasion of colorectal cancer cells. Mol Oncol. 2019;13(11):2393-2405. doi: 10.1002/1878-0261.12566.
47. Chang W, Gao W, Luo B, Chen Y, Wen Z. Comprehensive Insights Into the Role of TRPM4 in Pan-Cancer Progression and Immune Regulation. Immunotargets Ther. 2025;14:831-848. doi: 10.2147/ITT.S542176.
48. Chugh S, Gnanapragassam VS, Jain M, et al. Pathobiological implications of mucin glycans in cancer: sweet poison and novel targets. Biochim Biophys Acta. 2015;1856:211-225. doi:10.1016/j.bbcan.2015.08.003
49. Taniguchi T, Woodward AM, Magnelli P, et al. N-Glycosylation affects the stability and barrier function of the MUC16 mucin. J Biol Chem. 2017;292:11079-11090. doi:10.1074/jbc.M116.770123
50. Parry S, Hanisch FG, Leir SH, et al. N-Glycosylation of the MUC1 mucin in epithelial cells and secretions. Glycobiology. 2006;16:623-634. doi:10.1093/glycob/cwj110
51. Contessa JN, Bhojani MS, Freeze HH, et al. Inhibition of N-linked glycosylation disrupts receptor tyrosine kinase signaling in tumor cells. Cancer Res. 2008;68:3803-3809. doi:10.1158/0008-5472.CAN-07-6389
52. Lopez-Sambrooks C, Shrimal S, Khodier C, et al. Oligosaccharyltransferase inhibition induces senescence in RTK-driven tumor cells. Nat Chem Biol. 2016;12:1023-1030. doi:10.1038/nchembio.2194
53. Fanunza E, Frau A, Corona A, et al. Antiviral agents against Ebola virus infection: repositioning old drugs and finding novel small molecules. Annu Rep Med Chem. 2018;51:135-173. doi:10.1016/bs.armc.2018.08.004
54. Clarke EC, Nofchissey RA, Ye C, et al. The iminosugars celgosivir, castanospermine and UV-4 inhibit SARS-CoV-2 replication. Glycobiology. 2021;31:378-384. doi:10.1093/glycob/cwaa091
55. Sayce AC, Alonzi DS, Killingbeck SS, et al. Iminosugars inhibit dengue virus production via inhibition of ER alpha-glucosidases—not glycolipid processing enzymes. PLoS Negl Trop Dis. 2016;10:e0004524. doi:10.1371/journal.pntd.0004524
56. Almahayni K, Spiekermann M, Fiore A, et al. Small molecule inhibitors of mammalian glycosylation. Matrix Biol Plus. 2022;16:100108. doi:10.1016/j.mbplus.2022.100108
57. Banerjee S, Ansari AA, Upadhyay SP, Mettman DJ, et.al. Benefits and Pitfalls of a Glycosylation Inhibitor Tunicamycin in the

Therapeutic Implication of Cancers. Cells. 2024;13(5):395. doi: 10.3390/cells13050395.

58. Kopetz, S., Yoshino, T., Van Cutsem, E. et al. Encorafenib, cetuximab and chemotherapy in BRAF-mutant colorectal cancer: a randomized phase 3 trial. Nat Med 2025; 31, 901–908. https://doi.org/10.1038/s41591-024-03443-3
59. He H, Yuan J, Wang H, Chen L, et.al. L1TD1 promotes colorectal mucinous adenocarcinoma progression by enhancing ABCC3 mRNA stability. Oncogene. 2026;45(12):1071-1086. doi: 10.1038/s41388-026-03716-w.
60. Subramanian A, Narayan R, Corsello SM, Peck DD, et.al. A Next Generation Connectivity Map: L1000 Platform and the First 1,000,000 Profiles. Cell. 2017;171(6):1437-1452.e17. doi: 10.1016/j.cell.2017.10.049.